ISSN 2522-9818 (print)
ISSN 2524-2296 (online) *Innovative technologies and scientific solutions for industries. 2025. No. 3 (33)*

UDC 004.932.2 DOI: https://doi.org/10.30837/2522-9818.2025.3.088

YU. POHULIAIEV, K. SMELYAKOV

METHOD FOR COMPARING FINGERPRINTS BASED ON A PREVIOUS ALIGNMENT MODEL

The subject of this article is the development and analysis of a new method for comparing fingerprints that uses the geometric Euclidean characteristics of minutiae for biometric identification. The research focuses on minutiae – special points of interruption or bifurcation of papillary lines – as key biometric features, contrasting them with traditional global and local descriptors such as SIFT, HOG, or LPQ. The **purpose** of the **article** is to develop a robust and efficient fingerprint comparison method that uses Euclidean geometric characteristics of minutiae and pre-alignment to improve the accuracy of biometric identification without relying on machine learning. **The research task** was performed in three stages: first, studying the theoretical provisions of minutia-based descriptors and their invariance to affine transformations (shift, rotation, scaling); second, development of a model using a shift vector and distance functions for matching minutiae; third, experimental verification of the model, determination of optimal parameters, and evaluation on a standard data set. **Methods** include theoretical analysis and experimental evaluation. The theoretical basis establishes the stability of alignment to shifts. The descriptor is formed through minutiae coordinates, distance functions, and alignment optimization. An image processing algorithm with filtering and minutiae analysis is used to extract features. **The results** are achieved through experimental verification on the FVC2000 (DB1_B) dataset and demonstrate high performance, as evaluated by classification metrics and execution time. **Conclusions** indicate the theoretical and practical achievements of the research. The model demonstrates theoretical and practical resistance to Euclidean shifts, with advantages for processing prints from different scanners. Experiments confirm the effectiveness of shift detection, achieving a high Van Rijseberg score (0.735), although dependence on positive matches requires additional filtering of false positives. The method is workable and can be applied in practice.

Keywords: dactyloscopy; fingerprints; preliminary alignment; minutiae; biometric identification; affine transformations; tensor representation; machine learning; FVC2000; binary classification metrics.

Introduction

Dactyloscopy, which emerged as a science in the second half of the 19th century, remains relevant in the 21st century thanks to the uniqueness of papillary lines and the ease of obtaining prints. The study of the structure of fingerprints and the discovery of the exceptional properties and shapes of papillary patterns were carried out by British pioneers: Sir William James Herschel, a colonial administration official in Bengal; Henry Folds, a Scottish doctor in Japan; and Sir Francis Galton, a British researcher. Their work laid the foundation for the use of dactyloscopic methods in identification and forensics, ensuring significant competitiveness compared to the system proposed by French researcher and lawyer Alphonse Bertillon [1]. The greater resistance of fingerprints to change, combined with the ease of taking them compared to the Bertillonage procedure, gave fingerprinting an advantage in the 20th century, especially with the progress of computer technology.

One of the key milestones in the development of fingerprinting was the transition of criminalistics to automated fingerprint identification systems (AFIS) during the 1970s and 1980s, primarily in Western Europe and the United States. The evolution of computer technology, databases, and the ability to automatically search for image fragments without human intervention significantly accelerated the processing of biometric information and reduced storage resources – cumbersome fingerprint card indexes were replaced by electronic storage. The second important milestone was the improvement of computer vision tools and machine learning methods, which made it possible to study the details of papillary patterns in greater depth and expanded the variety of approaches to fingerprint matching. This has ensured the competitiveness of fingerprinting in the 21st century compared to new biometric methods such as facial or iris recognition.

Despite significant progress in fingerprinting in the 20th century, it faces a number of challenges that remain partially or completely unresolved even in the 21st century. Fingerprinting methods are sensitive to the quality of the prints, which depends on finger pressure, skin condition, or scanner performance. Issues of distortion (shifting, scaling, inversion, or rotation of prints) remain partially unresolved. Modern fingerprinting systems must meet requirements for quality and speed of results.

These features and contradictions confirm the relevance of developing new methods for recognizing and

Сучасний стан наукових досліджень та технологій в промисловості. 2025. № 3 (33)
ISSN 2522-9818 (print)
ISSN 2524-2296 (online)

comparing fingerprints. This study proposes a fingerprint comparison method based on the geometric Euclidean characteristics of minutiae and preliminary alignment for effective biometric identification with minimized distortion without the use of machine learning.

Analysis of the problem and existing methods

Recent works describe new problems and challenges in fingerprint processing and matching. For example, *Machado et al*. (2025) consider aspects of working with newborn fingerprints [2], while *Raj et al.* (2020) investigates the nature of latent fingerprints and their application [3]. Affine transformations, such as scaling, translation, and rotation, can significantly affect the quality of the system. *Guan et al.* (2025) investigated the problem of matching and aligning partial prints [4], while *Wang et al.* (2025) proposed a model to overcome these limitations, which includes not only the patterns of all fingers, but also the patterns of blood vessels (veins) [5]. This largely determines the divergence of methods for applying fingerprints and their processing. Equally important is the aspect of biometric ADIS performance, especially given the increasing prevalence of fingerprint scanners in consumer electronic devices. *Ravulakollu et al.* (2025) proposed a fast *few-shot* learning method for establishing and recognizing latent fingerprints [6].

The challenges outlined above for modern fingerprinting systems determine the variety of approaches used in current research. Structurally, they can be divided into the following groups: methods that use minutiae (or Galton points); methods based on the structure of fingerprint ridges; various models of fingerprint alignment (both with and without the introduction of machine learning methods); methods of comparing prints using machine learning methods, as well as other methods and models intended for limited use.

Methods based on minutiae are among the key ones in modern approaches to fingerprint comparison. Minutes (or Galton points) are specific points on a fingerprint that mark the beginning or end of one or more papillary lines. The most important points for study are the points where the papillary pattern is interrupted and the points where it splits. Their advantage is the uniqueness of the aggregate set and the relative ease of recognition, but minutiae are very sensitive to image artifacts and interference. *Maltoni et al*. (2009) systematized approaches to minutiae extraction, which have become the standard in fingerprinting [7]. *Ibragimov et al.* (2025) summarized pore detection methods (level 3) for latent and partial prints, proposing a basic detector and comparing it on the PolyU-HRF, L3-SF, and IITI-HRF datasets [8]. *Mani et al.* (2024) developed a two-stage authentication method that uses contour, edge, and line extraction with Euclidean distance and mutual information matching, achieving high accuracy [9].

Crest-based methods analyze the entire papillary pattern, unlike minutiae, which are only a unique structure of pattern intersections. On the one hand, this complicates processing, since it is necessary to extract specific lines rather than points. On the other hand, the pattern structure is more unique than a set of points and less prone to artifacts. Gu et al. (2006) proposed a method of combining ridges and minutiae, improving performance on FVC2002 [13]. *Li et al.* (2021) introduced a ridge pattern analysis algorithm that is robust to low image quality [14].

The next group of methods is alignment and correction of impressions. They are necessary for preliminary operations to extract ridges and minutiae most accurately. *Chen et al*. (2006) applied RANSAC for alignment based on coordinates and minutiae angles [10]. *Jain et al.* (2007) used orientation fields for coarse alignment at high resolution [11]. *Guan et al.* (2024) proposed a multi-task CNN transformer network for joint face verification and partial fingerprint alignment, improving accuracy on the NIST SD14 and FVC datasets [4]. *Dias et al.* (2025) developed a super-resolution method for newborn prints using *Vision Transformer*, improving noise-free details with a 10% increase in accuracy [2]. *Zhang et al.* (2022) implemented an optimized alignment algorithm that reduces computational costs [12].

Machine learning methods are presented in a significant number of studies. Their main advantage is their resistance to image artifacts and transformations, which makes these methods universal for working with images. The disadvantage is the high-performance requirements necessary for working with virtually any artificial intelligence model, which makes the development of high-performance machine learning-based models a priority. *Wang et al.* (2023) proposed a localized deep representation (LDRF) that combines alignment and feature extraction [15]. *Liu et al.* (2021) applied transformers for an interpretable fixed-length fingerprint representation [16]. *Kim et al.* (2022) developed hybrid neural networks that improve matching in noisy environments [17]. *Yang et al.* (2021) proposed a deep learning model for complex patterns that is resistant to deformations [18]. *Park et al.* (2020) implemented an algorithm that minimizes the impact of low image

ISSN 2522-9818 (print)
ISSN 2524-2296 (online) Innovative technologies and scientific solutions for industries. 2025. No. 3 (33)

quality [19]. *Ravulakollu et al.* (2025) applied *few-shot* learning with a prototype network based on DenseNet121 for latent fingerprint recognition, achieving an accuracy of 91.66% on the IIIT-D dataset [6].

The last group of methods has a narrow purpose. For the most part, they solve a specific problem, but the proposed approaches and solutions may also be of interest in the general context of matching and identification. *Zhao et al.* (2025) developed a technique for latent prints that improves identification at crime scenes [20]. *Xu et al.* (2025) proposed a method for partial prints based on local correlations [21]. *Lee et al.* (2024) implemented a secure matching protocol with encrypted information [22]. *Choi et al.* (2023) improved encryption protocols for biometric systems [23]. Wu et al. (2025) proposed a method for removing interfering minutiae from latent fingerprints [24]. *Han et al.* (2024) optimized computations for ADIS [25]. *Kim et al.* (2023) presented architectures for improving accuracy [26]. *Park et al.* (2023) developed deep learning for complex deformations [27]. *Lim et al.* (2020) implemented adaptive filtering for preprocessing [28]. *Sathya et al.* (2020) improved latent prints with linear feature extraction, achieving an accuracy of over 80% [3]. *Wulandari et al.* (2021) developed an identification system with edge detection and GLCM, achieving an accuracy of 83% [29]. *Patel et al.* (2021) proposed a technique for high-noise fingerprints [30]. *Wang et al.* (2024) created a contactless multimodal system for four-finger fingerprints and veins with the ACFNet network, achieving an EER of 0.07% [5]. *Yu et al.* (2025) implemented 3D fingerprint unfolding with B-spline for 2D recognition, with an EER ranging from 0.2072% to 1.50% [31]. *Calderón-Calderón et al.* (2025) proposed a method for improving the quality of prints for low-resolution scanners, increasing image clarity and facilitating feature extraction, which is particularly useful for inexpensive consumer devices [32].

A comparative analysis of the groups of methods is presented in Table 1.

Table 1. *Comparison of fingerprint matching methods*

Method	Features	Noise resistance	Accuracy, EER (%)	Computational complexity	Data nets
Minutiae	Galton points	low	1–2	low	FVC, PolyU-HRF
Rows	papillary patterns	medium	0.5–1	medium	FVC2002
Alignment	coordinates, orientation	medium	0.3–1	high	NIST SD14, FVC
Machine learning	deep features	high	0.4–1	very high	IIIT-D, NIST

Analysis of research confirms the relevance of developing new methods for comparing fingerprints using minutiae features. Machine learning methods are often cumbersome and unsuitable for simple application scenarios. However, it is necessary to take into account the problems outlined by the authors, in particular image artifacts during minutiae recognition, the need for preliminary alignment, etc. The proposed pre-alignment method is based on Euclidean characteristics of minutiae, minimizes the impact of affine transformations, and optimizes computational complexity, making it suitable for real-time applications.

Purpose and objectives of the research

The purpose of this research is to develop a robust and efficient fingerprint comparison method that uses Euclidean geometric features of minutiae and pre-alignment to improve the accuracy of biometric identification without relying on machine learning, ensuring computational efficiency and suitability for real-time operation in the presence of noise, artifacts, and affine transformations.

Research objectives:

– to analyze existing fingerprint processing methods, evaluate their robustness to noise, artifacts, and affine transformations such as shift, rotation, and scaling;

– to develop a mathematical model for fingerprint comparison based on pre-alignment, relying on tensor representation of images, shift vector, and minutiae matching using distance function and tolerance ratio;

– to implement a software solution for practical application of the model using image processing tools and high-performance computing;

– to perform experimental verification of the model on the standard FVC2000 (DB1_B) dataset using binary classification metrics and measure the execution time;

– to determine the optimal parameters to ensure a balance between the accuracy and performance of the method.

Fingerprint comparison method

Within the scope of the outlined research objectives and tasks, we propose to consider a method of comparing

ISSN 2522-9818 (print)
Сучасний стан наукових досліджень та технологій в промисловості. 2025. № 3 (33) ISSN 2524-2296 (online)

fingerprints based on a pre-alignment model. Earlier, we pointed to the problem of pre-alignment as one of the most important stages of biometric fingerprint matching. To this end, we present a mathematical model of the method.

Let there be a vector space V:

$$V \cong \mathbb{R}^3, \tag{1}$$

where $\mathbb{R}$ – field of real numbers.

Let's introduce the basis of the vector space V:

$$\begin{aligned} &\forall i \in [1,3] \cap \mathbb{Z} : \exists \mathbf{e}_i \in V \\ &\mathbf{e}_1 = (1,0,0) \\ &\mathbf{e}_2 = (0,1,0) \\ &\mathbf{e}_3 = (0,0,1), \end{aligned} \tag{2}$$

where $\mathbf{e}_i$ – basis vectors.

Then we define a pixel as a tensor of type (1, 0). Here and below, the notation $a^i b_i$ refers to Einstein's notation for tensors.

$$\forall p^i \in [0,255] \cap \mathbb{Z} : \mathbf{p} = p^i \mathbf{e}_i, \quad \mathbf{p} \in V, \tag{3}$$

where p^i – integer pixel components; $\mathbf{p}$ – first-order contravariant tensor.

Let's introduce vector spaces H i W:

$$\begin{aligned} H &= V\left\{ \mathbf{f}_m \middle| \forall m \in [1,M] \cap Z \right\}, \quad \mathbf{f}_m \in H, \\ W &= V\left\{ \mathbf{f}_n \middle| \forall n \in [1,N] \cap Z \right\}, \quad \mathbf{f}_n \in H, \end{aligned} \tag{4}$$

where V – linear span of vector space elements; $\mathbf{f}_m$ and $\mathbf{f}_n$ – basis space vectors; M and N – space dimensions (width and height).

Then we define the image as a tensor of type (3, 0):

$$\mathbf{P} = P^{mni}\left(\mathbf{f}_m \otimes \mathbf{f}_n \otimes \mathbf{e}_i\right), \quad P \in H \otimes W \otimes V, \tag{5}$$

where P^{mni} – image components; P – third-order contravariant tensor.

Within specific values of m and n, the image and pixel components are related:

$$\forall m,n,i : P^{mni} = p^i \ . \tag{6}$$

Since our method is based on the characteristics of minutiae, we will briefly describe their extraction (since we are working with a ready-made minutia detector). Here and further, we will understand minutia as a tuple of values from a mixed vector space:

$$\begin{aligned} M &= \mathbb{R}^2 \times S^1 \times T \\ S^1 &= \mathbb{R}/2\pi k \quad \forall k \in \mathbb{Z} \\ T &= \{0,1\} \\ m &= (x,y,\alpha,t) \quad \forall m \in M, \end{aligned} \tag{7}$$

where M – minutiae space; S^1 – factor set denoting the single circle of minutiae orientation angles; T – set of minutiae types (bifurcation or interruption); m – minutia itself is a set of four values.

Then the minutiae detector

$$\Phi : \mathbf{P} \to M, \tag{8}$$

where Φ – reproducing the image in minutiae space.

Since the pre-alignment model is available to us and works with a set of minutiae for an image, we will also describe it:

$$A : 2^M \times 2^M \to \mathbb{R}^2, \tag{9}$$

where A – reproducing the space of minutiae sets into a vector of image shifts relative to each other, 2^M – a set of all subsets.

Let us assume that, as a result of applying operators Φ and A, we obtain a shift vector s for two images $\mathbf{P}_1$ and $\mathbf{P}_2$. Then, the first step of the procedure will be to align the second image with the first one:

$$\begin{aligned} &\sigma_s : M \to N \\ &\sigma_s(m) = (x + \Delta x, y + \Delta y, \alpha, t), \end{aligned} \tag{10}$$

where σ_s is the image shift operator; Δx and Δy are components of vector s.

We assume that the shift model should correctly describe the same fingerprint under different affine transformations. However, this should imply the equivalence of two fingerprints. Therefore, we formulate the working hypothesis as follows:

$$\begin{aligned} &\forall \mathbf{P}_1, \mathbf{P}_2 \in \mathbf{P} : \exists s \in \mathbb{R}^2 : s = A\left(\Phi(\mathbf{P}_1), \Phi(\mathbf{P}_2)\right) \\ &\Phi(\mathbf{P}_1) \sim \sigma_s\left(\Phi(\mathbf{P}_2)\right) \leftrightarrow \mathbf{P}_1 = \mathbf{P}_2 \ , \end{aligned} \tag{11}$$

where $\sim$ is the equivalence relation between sets of minutiae, the criterion for which will be given below.

Therefore, we assume that if two sets of minutiae are equivalent after applying the calculated shift, then we are dealing with the same fingerprint. Given the structure of the minutiae tuple, we propose the following criterion for the equivalence of sets:

$$\begin{aligned} &\forall M_1, M_2 \subset M : \exists L \subset M : L = \begin{cases} M_1, |M_1| \le |M_2| \\ M_2, |M_1| > |M_2| \end{cases} \\ &\exists G \subset M : G = \left((M_1 \cup M_2)/L\right) \cup (M_1 \cap M_2), \\ &\exists C \in \mathbb{N}, C = \left| \left\{ m \in L \middle| \exists m_2 \in G : m \simeq m_2 \right\} \right| \\ &\frac{C}{|L|} \ge C_{threshold} \leftrightarrow M_1 \sim M_2 \ , \end{aligned} \tag{12}$$

where L is the smaller of the sets according to the power criterion; G is the larger of the sets according to the power criterion; C is the number of minutiae that satisfy the tolerance ratio; $\simeq$ is the tolerance ratio on the set of

ISSN 2522-9818 (print)
ISSN 2524-2296 (online) Innovative technologies and scientific solutions for industries. 2025. No. 3 (33)

minutiae; $C_{threshold}$ is the threshold value for the number of tolerant minutiae.

On the space of minutiae M, we define the distance function and the order relation:

$$\begin{gathered}\forall m_1=(x_1,y_1,\alpha_1,t_1),\ m_2=(x_2,y_2,\alpha_2 t_2)\in M: d(m_1,m_2)=|x_1-x_2|,|y_1-y_2|,\min_{k\in\mathbb{Z}}|\alpha_1-\alpha_2+2\pi k|,(t_1\odot t_2)\in M\\ S^1=\mathbb{R}/2\pi\mathbb{Z}=\left\{e^{i\theta}\,\middle|\,\theta\in\mathbb{R}\wedge e^{i\theta}=e^{i(\theta+2\pi k)}\forall k\in\mathbb{Z}\right\}\\ \exists\theta_0=0,\varphi(\alpha)=(\theta-\theta_0)\bmod 2\pi:\alpha_1\le\alpha_2\leftrightarrow\varphi(\alpha_1)\le\varphi(\alpha_2)\\ (x_1\le x_2)\wedge(y_1\le y_2)\wedge(\alpha_1\le\alpha_2)\wedge(t_1\vee\neg t_2)\leftrightarrow m_1\le m_2,\end{gathered}\tag{13}$$

where d is the distance function; $\odot$ is the XNOR operator; θ_0 is the starting reference angle; φ is the function that reduces the angle on the single circle to the range $[0,\ 2\pi)$. Then we set the tolerance ratio in the minutiae space:

$$\forall m_1,m_2\in M:\exists\Delta m\in M: d(m_1,m_2)\le\Delta m\leftrightarrow m_1\simeq m_2,\tag{14}$$

where Δm is the vector of permissible deviation during minutiae comparison.

It is easy to see that the definition given in formula (14) does indeed correspond to the tolerance ratio. It is reflexive:

$$\begin{gathered}\forall m,\Delta m\in M: d(m,m)=\mathrm{i}(\mathrm{nf}\,\mathbb{R}_{+0},\inf\mathbb{R}_{+0},\inf[0,2\pi),\inf\{0,1\})\\ \forall Q,q\in Q:\inf Q\le q\to d(m,m)\le\Delta m\to m\simeq m,\end{gathered}\tag{15}$$

symmetrical:

$$\begin{gathered}\forall m_1,m_2,\Delta m\in M:|x|=|-x|\to d(m_1,m_2)=d(m_2,m_1)\\ d(m_1,m_2)\le\Delta m\to d(m_2,m_1)\le\Delta m\\ (m_1\simeq m_2)\leftrightarrow(m_2\simeq m_1)\end{gathered}\tag{16}$$

At the same time, the relationship is not transitive:

$$\begin{gathered}\forall m_1,m_2,m_3,\Delta m\in M:\left(d(m_1,m_2)\le\Delta m\wedge d(m_2,m_3)\le\Delta m\not\to d(m_1,m_3)\le\Delta m\right)\\ \left((m_1\simeq m_2)\wedge(m_2\simeq m_3)\right)\not\leftrightarrow(m_1\simeq m_3).\end{gathered}\tag{17}$$

The procedure proposed in formula (12) does not guarantee optimality under the condition of a shift search model found. Moreover, a situation may easily arise when a threshold value that is not selected accurately enough will cut off the correct pair of minutiae sets. Therefore, it is necessary to verify the optimality of the result.

We set the reproduction that takes into account specific pairs of minutiae matched in formula (12):

$$\begin{gathered}S:M\times M\to J,\quad J\subset\mathbb{R}^2:|J|=C/|L|\\ S(M_1,M_2)=\left\{m_1\in L\,\middle|\,\exists!m_2\in G:(m_1\simeq m_2)\wedge\left(O(m_1,G)=m_2\right)\right\}\to\left\{\delta(m_1,m_2)\right\}\end{gathered}\tag{18}$$

where O is the optimal matching search function; δ is the Euclidean distance function between minutiae.

The description of the optimal matching search function should begin with the introduction of the minutiae similarity metric. Above, in formula (14), the tolerance ratio is specified, which allows us to distinguish between previously matching minutiae and non-matching minutiae. However, in the process of completely enumerating pairs among two sets of minutiae, we cannot guarantee that each minutia of the first set corresponds bijectively to only one minutia of the second set. Then we will define the minutiae similarity function:

$$\begin{gathered}\forall m_1,m_2,\Delta m\in M:\exists M_d\subset\mathbb{R}\times[0,\pi]\times T,\gamma:M\to M_d\\ \gamma(m)=\left(\sqrt{x^2+y^2},\varphi(\alpha),t\right)=(\rho,\beta,t)\\ \forall m_d\in M_d:\varepsilon(m_d)=\left(1/\sqrt{x2+y2},1/\alpha,t\right)\\ \forall m_{d1},m_{d2}\in M_d\exists\eta:M_d\times M_d\to\mathbb{R}_{+0}\cup\{+\infty\}\\ \eta(m_{d1},m_{d2})=\rho_1\cdot\rho_2+\beta_1\cdot\beta_2+(\neg t_1\wedge t_2)\\ \lambda(m_1,m_2)=\begin{cases}\eta\left(\gamma\left(d(m_1,m_2)\right),\gamma\left(\varepsilon(\Delta m)\right)\right), m_1\simeq m_2\\ +\infty, m_1\not\simeq m_2\end{cases}\end{gathered}\tag{19}$$

where M_d is the minutiae space with the transformation of coordinate components into distance; γ is the function that converts coordinate components and angle; ε is the function that returns a vector of values for normalization; η is the function of scalar multiplication of minutiae; λ is the similarity function.

Сучасний стан наукових досліджень та технологій в промисловості. 2025. № 3 (33)
ISSN 2522-9818 (print)
ISSN 2524-2296 (online)

Given the definitions in formulas (13) and (14), we are interested in minimizing the value of the function, since this will mean the most accurate match of two minutiae in the case of $\lambda = 0$. The worst match of minutiae will be described by the value $\lambda = 1$, and in the case of a mismatch, the function will have a value of positive infinity.

Then the function for finding the optimal match looks like this:

$$\forall M_1, M_2 \subset M, m_1 \in M_1 : O(m_1, M_2) = \arg\min_{m2 \in M2} \lambda(m_1, m_2) \quad (20)$$

Then we set a recursive description of the result search function:

$$R(M_1, M_2) : M \times M \to \mathbb{N} \cup \{0\}$$

$$R(M_1, M_2) = \max_{B \in \{S(M_1, \sigma_s(M_2))\} \cup \{S(M_1, \sigma_\delta(M_2)) | \forall \delta \in S(M_1, \sigma_s(M_2))\}} |B|, \quad (21)$$

where B is all possible shift options obtained based on the results of matching minutiae pairs; s is the initial shift parameter found using the A ratio (see formula (11)).

Then the result of the method is the following ratio:

$$\forall M_1, M_2 \subset M : \frac{R(M_1, M_2)}{|L|} \geq C_{threshold} \leftrightarrow M_1 \sim M_2. \quad (22)$$

Therefore, within the framework of the working hypothesis, we assume that if the number of optimal minutiae matches in relation to the power of the smaller of the two minutiae sets exceeds a certain threshold value, we consider these two minutiae sets (and, therefore, the two fingerprints) to be equivalent. The proposed comparison scheme takes into account both possible affine transformations of images (using a pre-alignment model) and various detection situations (differences in artifacts, image quality, etc.).

Program implementation

The proposed mathematical model for comparing fingerprints, which uses preliminary alignment and minutiae analysis, can be implemented as a multi-module software system. The software provides the phases described in formulas (1)–(22), which facilitates image processing, feature extraction, and comparison, taking into account affine transformations and quality discrepancies.

The following technologies have been implemented for this purpose: Python and OpenCV for image processing, C# for high-performance computing, and ASP.NET for module integration and user interface interaction. This contributes to the efficiency and flexibility required for real-time applications [33].

Below is the module structure.

1. The image preprocessor converts the input scan images of fingerprints, presented as third-order tensors **P** (formula (5)), into a form suitable for analysis. Noise filtering, brightness normalization, and contrast enhancement of papillary lines are performed using OpenCV algorithms such as Gaussian smoothing and adaptive binarization. This minimizes the impact of artifacts related to skin quality, finger or scanner pressure, preparing images P_1 and P_2 for further detection. An example of the detector and preprocessor in action is shown in Figures 1 and 2.

Fig. 1. First scan image of fingerprint

Fig. 2. Second scan image of fingerprint

2. The minutiae detector implements the reproduction of Φ (formula (8)), extracting minutiae – special points of prints, such as interruptions and bifurcations of papillary lines. Each minutia is represented by a tuple m (formula (7)), where x, y are coordinates; α is the orientation angle; t is the type. An open detector based on skeletonization and local analysis algorithms from OpenCV is used. The result is sets of minutiae for images P_1 and P_2, shown in Figures 3 and 4 for a pair from the FVC2000 (DB_1B) dataset.

ISSN 2522-9818 (print)
ISSN 2524-2296 (online)

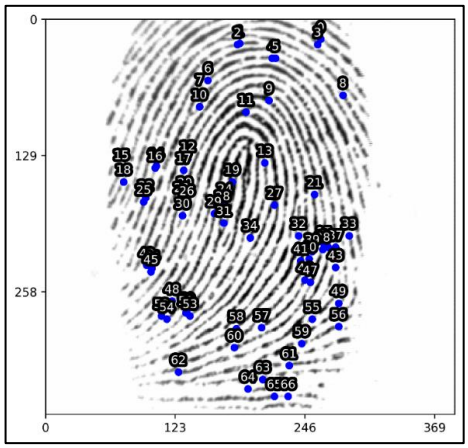

Fig. 3. Results of detecting the first scan image of the fingerprint

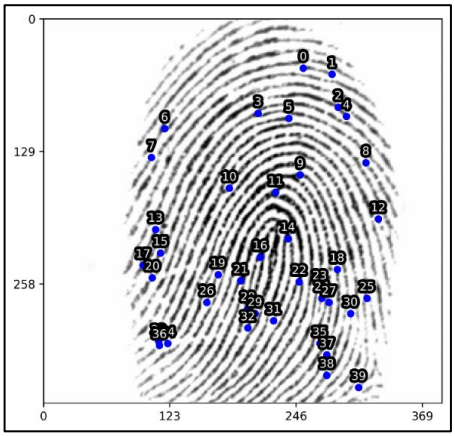

Fig. 4. Results of detecting the second scan image of the fingerprint

3. The alignment model implements the mapping A (formula (9)), calculating the shift vector s for aligning the images. Based on the minutiae sets, the coordinates and orientations are analyzed, and the optimal shift is determined. The Python implementation uses NumPy for efficient computations. The operator σ_s (formula (10)) is applied to image P_2, correcting its position relative to P_1. This compensates for the affine distortions observed in Figures 1 and 2.

4. The fingerprint matching method is implemented as a separate module and works with matching indices, calculating the distance function d (formula (13)) and similarity λ (formula (19)) for pairs of minutiae from sets L and G. The tolerance ratio $\simeq$ (formula (14)) cuts off mismatched pairs, taking into account the permissible deviations $\gamma(\Delta m)$. The function λ minimizes deviations in coordinates, angles, and minutiae types. Implementation in C# ensures high performance, and integration with Python via API allows the use of numerical libraries for tensor operations. The equivalence criterion (formula (12)) and the search for the optimal match O (formula (20)) are also implemented. Based on the shift vector s and a recursive approach (formula (21)), pairs of matching minutiae are determined by minimizing λ. The ratio (formula (22)) compares the number of optimal matches C with the threshold value $C_{threshold}$, confirming the equivalence of the prints. For a pair of images from FVC2000 (DB_1B) (see Figs. 1 and 2), the similarity score was 0.62 (in the range of 0–1), which preliminarily confirms the satisfactory performance of the method. The module is implemented on ASP.NET for integration with databases and the interface.

Hardware implementation

To ensure reliable results and efficient processing, all experiments were performed on a high-performance computing system. A workstation with an Intel Core i9-13900K processor (24 cores, 32 threads, base clock speed of 3.0 GHz, maximum clock speed of 5.8 GHz) and 64 GB of DDR5 RAM running at 5,200 MHz formed the basic hardware configuration. A 2 TB NVMe SSD was used for fast data transfer and access. To ensure compatibility with the software frameworks used in the experiments, the system was configured to run on Windows 11 Pro Build 26100.

Planning and description of experiments

The experiments in this study used the *Fingerprint Verification Competition* (FVC2000) DB1_B dataset, which is recognized as the gold standard for evaluating fingerprint recognition systems. Launched during the first fingerprint verification competition, the FVC2000 dataset is highly regarded in the field of biometric research for its consistent data collection methods and diverse fingerprint samples. The DB1_B subset was specifically selected for this study because it is small in size and suitable for evaluating algorithm productivity under controlled conditions.

The FVC2000 DB1_B dataset contains fingerprints captured using an inexpensive KeyTronic optical sensor with a resolution of 500 dpi. This dataset contains fingerprints from 10 individuals, each of whom provided eight prints from the same finger, for a total of 80 fingerprint images. The images are stored in 8-bit

Сучасний стан наукових досліджень та технологій в промисловості. 2025. № 3 (33)
ISSN 2522-9818 (print)
ISSN 2524-2296 (online)

grayscale format with a size of 300×300 pixels. The collection covers numerous fingerprint attributes, including varying degrees of line clarity, orientation, and inherent variations resulting from finger position or pressure.

The fingerprint scans in DB1_B were obtained under semi-controlled conditions, without strict regulations regarding finger placement or pressure, resulting in internal heterogeneity in the dataset. The optical sensor in DB1_B generates images that are characterized by moderate noise and sporadic artifacts, such as spots or incomplete ridge patterns, which complicates feature extraction and matching algorithms. These characteristics make DB1_B particularly suitable for evaluating the robustness of fingerprint recognition technologies to practical anomalies.

The dataset is publicly available and complies with the FVC2000 standard, which ensures consistency in data format and evaluation criteria across different research studies. Each photograph is given a unique identifier that indicates the person number and fingerprint number (e.g., "101_1.tif" for the first fingerprint of the first subject), which improves information management and research reproducibility.

The main objective of the experiments is to determine the optimal value of the tuple of minutiae threshold deviations $\gamma(\Delta m)$, the threshold value $C_{threshold}$, and to evaluate the performance of the method as a whole. To do this, we will use single-factor analysis methods and evaluate using binary classification metrics – assuming that each pair of images belongs to either the "match" class or the "mismatch" class. Accordingly, by calculating the derivative metrics of binary classification, we will be able to evaluate the performance of the method as a whole. We will conduct an experiment in an "all against all" format, i.e., each image in the dataset will be compared with all the others. With a dataset size of 80 images, we will perform 6,400 comparisons and obtain 6,400 results of the method's performance.

We propose the following metrics to study the productivity of the proposed method: primary metrics of binary classification (true positives, true negatives, false positives, false negatives), as well as derivative metrics such as: false positive rate (FPR), Van Rijsbergen's skewed measure with a coefficient of $\beta = 0.5$ $\left(F_\beta\right)$, Matthews correlation coefficient, which is a special case of Pearson's correlation coefficient (PCC), balanced accuracy measure (*Balanced Accuracy*), as well as the method's runtime. This focus on balanced metrics and metrics for evaluating the contribution of false positive results is due to the research area – from the point of view of the authentication task, a false positive result is less desirable than a false negative, since an unauthorized access error is significantly worse than an access error in general.

A detailed description of the primary metrics is proposed to be considered as follows:

$$\begin{gathered}\forall \mathbf{P}_1, \mathbf{P}_2 \in P : R_{12} = \left(\frac{R\left(M_1, M_2\right)}{|L|} \geq Cthreshold \right) \\ TP = R_{12} \wedge \left(\mathbf{P}_1 \sim \mathbf{P}_2\right) \\ FP = R_{12} \wedge \left(\mathbf{P}_1 \nsim \mathbf{P}_2\right) \\ FN = \neg R_{12} \wedge \left(\mathbf{P}_1 \sim \mathbf{P}_2\right) \\ TN = \neg R_{12} \wedge \left(\mathbf{P}_1 \nsim \mathbf{P}_2\right)\end{gathered} \tag{23}$$

where R_{12} is the comparison result for two images according to formula (22); TP is the measure of true positive results; FP is the measure of false positive results; TN is the measure of true negative results; FN is the measure of false negative results.

It is proposed to consider the derived metrics as follows:

$$\begin{gathered}P = TP/\left(TP + FP\right) \\ R = TP/\left(TP + FN\right) \\ F_\beta = \frac{\left(1+\beta^2\right) \cdot P \cdot R}{\beta^2 \cdot P + R} \in [0,1] \\ MCC = \frac{TP \cdot TN - FP \cdot FN}{\sqrt{\left(TP + FP\right) \cdot \left(TP + FN\right) \cdot \left(TN + FP\right) \cdot \left(TN + FN\right)}} \in [-1,1] \\ FPR = \frac{FP}{FP + TN} \in [0,1] \\ BAC = \frac{R + 1 - FPR}{2} \in [0,1],\end{gathered} \tag{24}$$

ISSN 2522-9818 (print)
ISSN 2524-2296 (online)
Innovative technologies and scientific solutions for industries. 2025. No. 3 (33)

where P is the positive prediction rate; R is the completeness measure; F_β is the shifted Van Rijsenberg measure; MCC is the Matthews correlation coefficient; FPR is the false positive prediction rate; BAC is the balanced accuracy.

Results

The first experiment was designed to determine the optimal threshold distance Δd . Table 2 shows the results of the experiment to study the distance component of the permissible deviation of minutiae.

Table 2. *Method productivity metrics depending on the permissible deviation of the distance component*

Testing №	Δd	F_β	MCC	FPR	BAC	Time (ms)
1	3	0.437	0.35	0	0.567	29155
2	6	0.536	0.415	0	0.594	42245
3	9	0.613	0.471	0	0.62	66942
4	12	0.689	0.535	0.0007	0.657	69515
5	15	0.735	0.586	0.003	0.697	111973
6	18	0.706	0.575	0.01	0.714	153514
7	21	0.635	0.539	0.024	0.729	141679
8	24	0.567	0.506	0.043	0.744	146207
9	27	0.499	0.47	0.068	0.753	179326
10	30	0.426	0.417	0.101	0.749	190190

For clarity, we will also illustrate the results obtained using graphs (see Figs. 5 and 6).

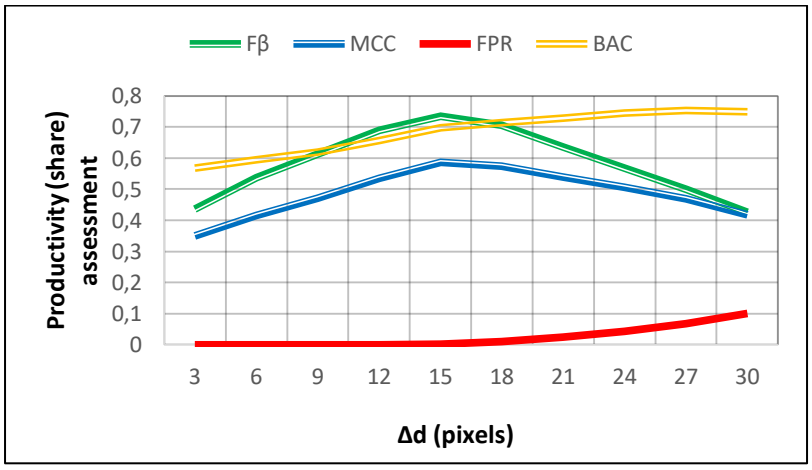

Fig. 5. Graphs of fluctuations in experimental values from experiment No. 1

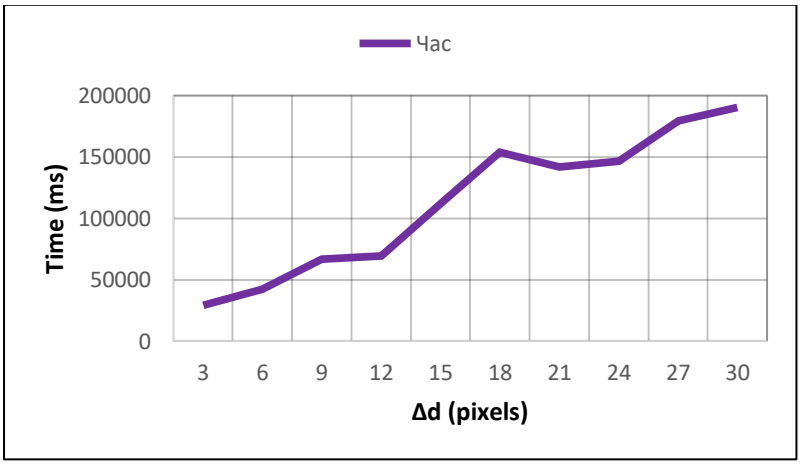

Fig. 6. Graph showing the dependence of the method's operating time on the distance limit

Сучасний стан наукових досліджень та технологій в промисловості. 2025. № 3 (33)
ISSN 2522-9818 (print)
ISSN 2524-2296 (online)

Several important conclusions can be drawn from the first experiment. First, the overall performance of the model has been preliminarily confirmed – a significant Van Rijsbergen measure result has been obtained (0.735 in the best case), and this performance is also illustrated by other metrics – the highest correlation coefficient and balanced accuracy measure. Second, the naive assumption about finding the optimal boundary distance has been experimentally confirmed – the graph line resembles a Gaussian and has an optimal value approximately in the middle of the range of definition. Third, the experiment demonstrates an increase in computational complexity in accordance with an increase in the boundary distance. This follows directly from the features of the procedure presented in formula (21). Since we are trying to find the optimal result by adding additional shifts, the number of these additional iterations directly depends on how many positive identification results we return. Interestingly, the main increase in time costs occurs in the middle of the range of definition, while before and after it we see either a more gradual increase or even a decrease in execution time (as shown in sections (18) – (21)). Fourth, the only metric that deviates from the trend is the balanced accuracy BAC (it begins to decline significantly later than the optimal threshold distance). However, there is an explanation for this: the accuracy metric takes into account the contribution of both false positive growth and true positive growth. Depending on how we see the growth of the false positive rate, the balanced accuracy metric will increase to the extent that the growth of the true positive rate exceeds the growth of the false positive rate. Both of these increases directly result from the fact that the number of false negatives decreases as the threshold value increases, thereby increasing the true positive and false positive results.

The second experiment was designed to determine the optimal threshold angle $\Delta\alpha$. Table 3 shows the results of the experiment to study the angle component of the permissible deviation of minutiae.

For clarity, we will also illustrate the results obtained using graphs (see Figs. 7 and 8).

Table 3. Productivity metrics of the method depending on the permissible deviation of the angle component

Testing №	Δα	F_β	MCC	FPR	BAC	Time (ms)
1	3	0.475	0.374	0	0.577	47858
2	6	0.609	0.468	0	0.619	67279
3	9	0.693	0.54	0.002	0.666	86475
4	12	0.735	0.586	0.003	0.697	131448
5	15	0.732	0.589	0.005	0.705	98835
6	18	0.691	0.566	0.012	0.714	134568
7	21	0.658	0.55	0.019	0.723	190983
8	24	0.625	0.531	0.026	0.728	193243
9	27	0.602	0.515	0.03	0.727	155286
10	30	0.564	0.491	0.039	0.727	165305

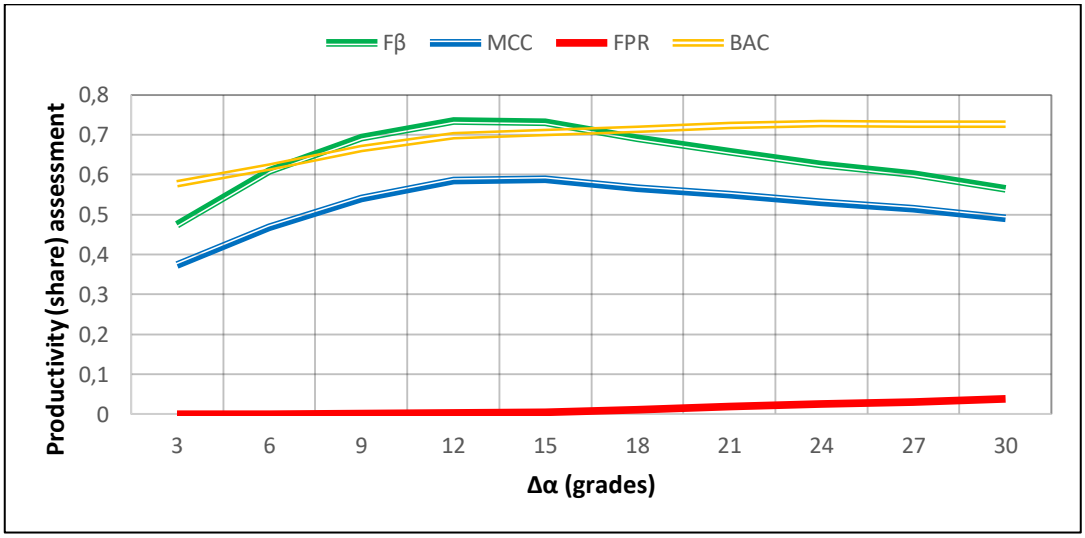

Fig. 7. Graphs of fluctuations in experimental values from experiment No. 2

ISSN 2522-9818 (print)
ISSN 2524-2296 (online)
Innovative technologies and scientific solutions for industries. 2025. No. 3 (33)

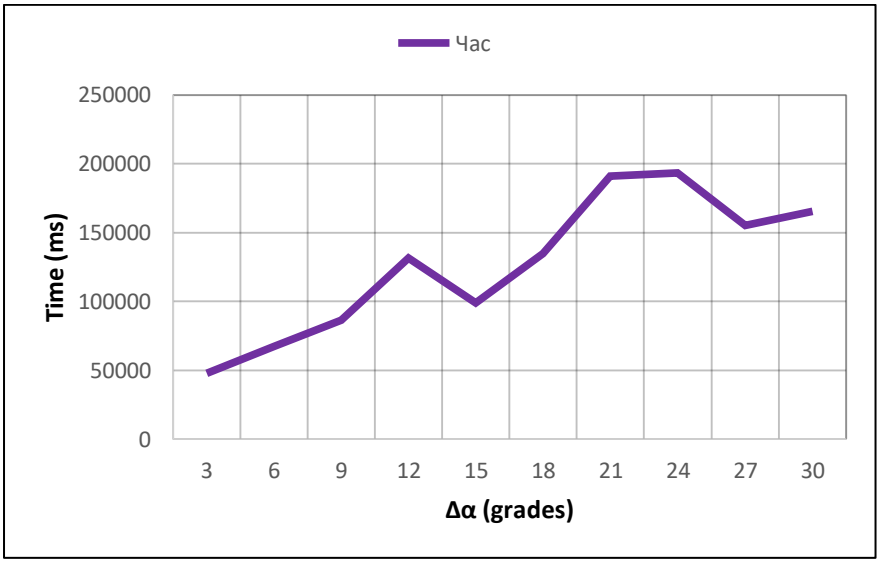

Fig. 8. Graph showing the dependence of the method's operating time on the threshold angle value

The second experiment largely confirms the results of the first – the graphs and trends are approximately the same. The optimal angle is closer to the center of the range of definition, and abnormal behavior in the method's execution time was noted during the experiment. This confirms the nonlinear dependence of the method's complexity on the thresholds and the number of images being processed.

The third experiment was designed to find the optimal value for minutiae type matching. Table 4 shows the results of the experiment studying the minutiae type component of the minutiae tolerance vector**.**

Table 4. *Productivity metrics of the method depending on the permissible deviation of the minutiae component*

Testing №	Δt	F_β	MCC	FPR	BAC	Time (ms)
1	0	0.733	0.583	0.003	0.695	103078
2	1	0.735	0.586	0.003	0.697	105674

The third experiment confirms the need to include minutiae type comparison in the method – under other equal conditions (such as false positive rate and execution time), the main indicators are better. That is, it is necessary to add minutiae type to the analysis.

Thus, the optimal value of the deviation vector component is $\gamma(\Delta m) = (15,\ 12,\ 1)$.

The fourth experiment was designed to find the optimal threshold value $C_{threshold}$. Table 5 shows the results of the experiment to find the optimal threshold value.

Table 5. *Productivity metrics of the method depending on the threshold value*

Testing №	$C_{threshold}$	F_β	*MCC*	*FPR*	*BAC*
1	1	0.417	0.338	0	0.5625
2	0.9	0.43	0.346	0	0.566
3	0.8	0.463	0.366	0	0.57
4	0.7	0.53	0.411	0	0.592
5	0.6	0.65	0.5	0.0003	0.637
6	0.5	0.735	0.586	0.003	0.697
7	0.4	0.652	0.556	0.023	0.737
8	0.3	0.465	0.455	0.088	0.764
9	0.2	0.225	0.258	0.377	0.712
10	0.1	0.136	0.107	0.864	0.559

For clarity, we will also illustrate the results obtained using a graph (see Fig. 9).

Therefore, the optimal threshold value is $C_{threshold} = 0.5$ or 50% of correct minutiae from the total number. Any lower threshold value begins to lead to an overly sharp disproportionate increase in the false positive rate.

Empirical studies confirm the effectiveness of the proposed method and demonstrate the correctness of the proposed working hypothesis regarding the equivalence of fingerprints. The result achieved is high enough for the practical application of such a model.

Сучасний стан наукових досліджень та технологій в промисловості. 2025. № 3 (33)
ISSN 2522-9818 (print)
ISSN 2524-2296 (online)

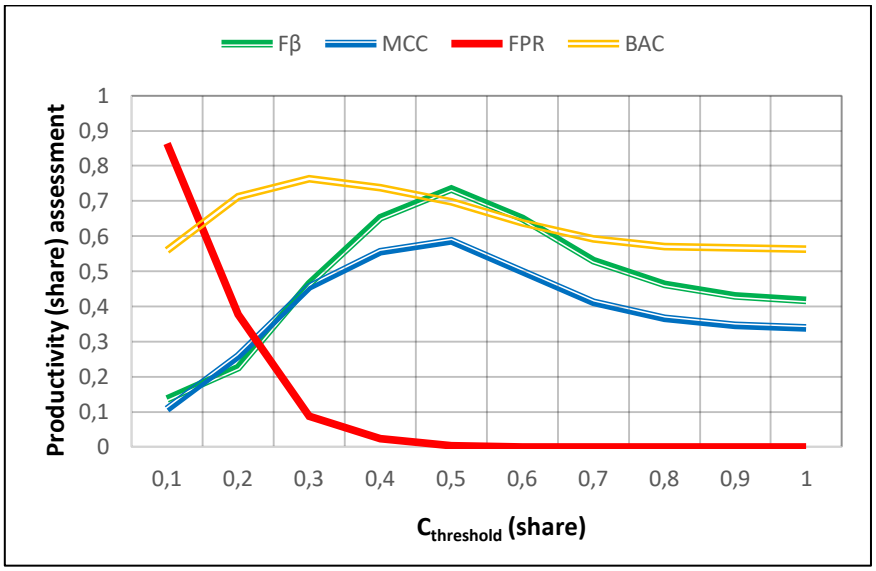

Fig. 9. Graphs of fluctuations in experimental values from experiment No. 4

Conclusions

Within the scope of the study, an original method for comparing fingerprints was proposed, based on a model of preliminary alignment and analysis of minutiae (characteristic points of papillary lines), which compensates for affine distortions by calculating a shift vector and determines the equivalence of prints through tolerance ratios and optimized minutiae matching. The mathematical model represents fingerprint images as third-order tensors in vector space, describes minutiae as tuples in mixed space considering coordinates, orientation angles, and types (breaks or bifurcations), and evaluates the equivalence of minutiae sets using a distance function, tolerance ratio, and minimization of deviations during matching.

The method is implemented as a multi-module system using Python and OpenCV for image processing, C# for high-performance computing, and ASP.NET for module integration on the FVC2000 (DB_1B) dataset. Experimental testing was performed on the specified set, which contains 80 images from 10 subjects with a resolution of 500 dpi, under conditions that simulate real scenarios with noise and artifacts, using 6400 comparisons in an "all against all" format, resulting in the following optimal parameters: vector of permissible deviation of minutiae $\left(\gamma(\Delta m) = (15,\ 12,\ 1)\right)$ for distance, angle, and type, as well as threshold value $\left(C_{threshold} = 0.5\right)$. The maximum Van Rijsbergen measure is 0.73, confirming the method's performance, while metrics such as the Matthews correlation coefficient, balanced accuracy, and false positive rate show satisfactory results.

The proposed method is characterized by resistance to affine distortions and artifacts, as well as low computational complexity, which ensures its suitability for real-time tasks and prospects in biometric systems. It is also worth noting that, despite the potential for complete resistance to affine transformations, this study focuses only on Euclidean shifts. Potential improvements may include accounting for the rotation angle of two images and the scaling effect.

References

1. Sengoopta, C. (2004), *Imprint of the Raj: how fingerprinting was born in colonial India.* London, Pan, 234 p.
2. Machado, J. H. P., Koop, B. D. O., Filipak, M., Barbosa, M. A. C., Oliva, J. T. Southier, L. F. P. (2025), "A Super-Resolution Approach for Image Resizing of Infant Fingerprints With Vision Transformers". *IEEE Access*, Vol. 13, P. 67718–67728. DOI: 10.1109/ACCESS.2025.3561206
3. Raj, J. M., Rakshitha, S., Priya, S. S., Vaishnavi, S. & Sivaranjani, A. (2020), "Latent Fingerprint Enhancement for Investigation". *2020 6th International Conference on Advanced Computing and Communication Systems (ICACCS)*, Coimbatore, India, IEEE, P. 644–648. DOI: 10.1109/ICACCS48705.2020.9074191

4. Guan, X., Pan, Z., Feng, J. & Zhou, J. (2025), "Joint Identity Verification and Pose Alignment for Partial Fingerprints". *IEEE Transactions on Information Forensics and Security*, Vol. 20, P. 249-263. DOI: 10.1109/TIFS.2024.3516566
5. Wang, S., Shen, Y. Yang, W. (2025), "Touchless Finger Vein and Fingerprint Verification via Exploiting Attention-Based Cross-Domain Fusion". *IEEE Transactions on Circuits and Systems for Video Technology*, Vol. 35, No. 4, P. 3426–3437. DOI: 10.1109/TCSVT.2024.3504270
6. Ravulakollu, K. K., Reddy, G. S. N., Jadhav, M., Batti, V., Vupputuri, V. K. Polishetty, R. K. (2025), "Limited Training Approach To Model Latent Fingerprint Data For Time-Constrained Solutions". *2025 17th International Conference on COMmunication Systems and NETworks (COMSNETS)*, Bengaluru, India, IEEE, P. 90–95. DOI: 10.1109/COMSNETS63942.2025.10885690
7. Maltoni, D., Maio, D., Jain, A.K. & Prabhakar, S. (2009), "Handbook of Fingerprint Recognition". *2nd ed. London, Springer*, 496 p. DOI: 10.1007/978-1-84882-254-2
8. Ibragimov, A., Ferreira, F. Santos, G. (2025), "Fingerprint Pore Detection: A Survey and Comparative Analysis". *IEEE Transactions on Biometrics, Behavior, and Identity Science*, Vol. 7, No. 1. DOI: 10.1109/TBIOM.2025.3560655
9. Mani, K., Kumar, R., Singh, P. Sharma, A. (2024), "Two-Step Fingerprint Authentication Using Contour and Edge Matching". *2024 International Conference on Advanced Computer Information Technologies (ACIT)*, Rzeszow, Poland, IEEE, P. 123–128. DOI: 10.1109/ACIT62805.2024.10877179
10. Chen, L., Moon, Y.S. Lee, H.K. (2006), "Efficient Alignment of Fingerprint Images". *2006 IEEE International Conference on Image Processing*, Atlanta, GA, USA, IEEE, P. 169–172. URL: https://ieeexplore.ieee.org/document/1698755 (last accessed 01.05.2025).
11. Jain, A.K., Feng, J. Nandakumar, K. (2007), "Orientation Field Alignment for Fingerprint Matching". *Advances in Biometrics: International Conference, ICB 2007*, Seoul, South Korea, Springer, P. 745–754. DOI: 10.1007/978-3-540-74549-5_75
12. Zhang, Y., Li, X. & Wang, H. (2022), "Optimized Fingerprint Alignment for Large-Scale Databases". *2022 IEEE International Conference on Systems, Signals and Image Processing (IWSSIP)*, Sofia, Bulgaria, IEEE, P. 1–4. DOI: 10.1109/SILCON55242.2022.10028828
13. Gu, J., Zhou, J. Zhang, C. (2006), "Fingerprint Matching Using Ridges". *Pattern Recognition*, Vol. 39, No. 11, P. 2131–2140. DOI: 10.1016/j.patcog.2006.04.015
14. Li, X., Zhang, Y. Chen, L. (2021), "Ridge Pattern Analysis for Low-Quality Fingerprint Images". *2021 International Conference on Smart Cities and Energy Efficiency (ICSCEE)*, Istanbul, Turkey, IEEE, P. 1–6. DOI: 10.1109/ICSCEE50312.2021.9497996
15. Wang, H., Li, Y. Zhang, X. (2023), "Localized Deep Representation for Fingerprint Matching". *arXiv preprint arXiv:2311.18576v2*, 15 p. URL: https://arxiv.org/html/2311.18576v2 (accessed 01.05.2025)
16. Liu, Z., Zhang, Q. Wang, S. (2021), "Transformer-Based Fingerprint Representation for Matching". *IEEE Transactions on Information Forensics and Security*, Vol. 16, P. 4867–4878. DOI: 10.1109/TIFS.2021.3134867
17. Kim, S., Park, J. Lee, H. (2022), "Hybrid Neural Networks for Fingerprint Matching in Noisy Conditions". *2022 International Conference on Future Trends in Intelligent Computing (ICFTIC)*, Shanghai, China, IEEE, P. 45–50. DOI: 10.1109/ICFTIC57696.2022.10075139
18. Yang, J., Chen, X. Zhang, L. (2021), "Deep Learning for Complex Fingerprint Patterns". *IEEE Transactions on Information Forensics and Security*, Vol. 16, P. 3921–3932. DOI: 10.1109/TIFS.2021.3139219
19. Park, T., Kim, Y. Lee, S. (2020), "Algorithm for Low-Quality Fingerprint Image Matching". *2020 International Conference on Systems, Signals and Image Processing (IWSSIP)*, Niteroi, Brazil, IEEE, P. 123–128. DOI: 10.1109/ICSSIT48917.2020.921420
20. Zhao, Q., Li, J. Wang, X. (2025), "Latent Fingerprint Processing for Crime Scene Identification". *2025 IEEE Workshop on Applications of Computer Vision (WACV Workshops)*, Tucson, AZ, USA, IEEE, P. 56–61. DOI: 10.1109/WACVW65960.2025.00159
21. Xu, L., Zhang, Y. Chen, H. (2025), "Local Correlation-Based Matching for Partial Fingerprints". *IEEE Access*, Vol. 13, P. 12345–12354. DOI: 10.1109/ACCESS.2025.3555311
22. Lee, H., Kim, S. Park, J. (2024), "Secure Protocol for Fingerprint Matching with Encrypted Data". *IEEE Transactions on Pattern Analysis and Machine Intelligence*, Vol. 46, No. 8, P. 5678–5690. DOI: 10.1109/TPAMI.2024.3486179
23. Choi, Y., Lee, H. Kim, D. (2023), "Enhanced Encryption Protocols for Biometric Systems". *2023 International Conference on Biometrics and Signal Processing (BIOSIG)*, Darmstadt, Germany, IEEE, P. 89–94. DOI: 10.1109/BIOSIG58226.2023.10345974
24. Wu, X., Zhang, L. Chen, Y. (2025), "Obstructive Minutiae Removal for Latent Fingerprints". *IEEE Sensors Letters*, Vol. 9, No. 3, P. 1–4. DOI: 10.1109/LSENS.2025.3550874
25. Han, C., Li, X. Wang, Y. (2024), "Optimized Computations for Automated Fingerprint Identification Systems". *2024 International Conference on Systems and Electronics (ICSES)*, Singapore, IEEE, P. 34–39. DOI: 10.1109/ICSES63445.2024.10763052
26. Kim, D., Park, J. Lee, S. (2023), "New Architectures for Fingerprint Recognition Accuracy". *2023 Asia-Pacific Signal and Information Processing Association Annual Summit and Conference (APSIPA ASC)*, Taipei, Taiwan, IEEE, P. 123–128. DOI: 10.1109/APSIPAASC58517.2023.10317455
27. Park, J., Kim, Y., Lee, H. (2023), "Deep Learning for Complex Fingerprint Deformations". *2023 IEEE International Conference on Artificial Intelligence Circuits and Systems (AICAS)*, Hangzhou, China, IEEE, P. 56–61. DOI: 10.1109/AICAS57966.2023.10168628
28. Lim, S., Chen, X., Zhang, Y. (2020), "Adaptive Filtering for Fingerprint Preprocessing". *2020 IEEE International Conference on Advances in Science, Engineering and Technology (ASET)*, Dubai, UAE, IEEE, P. 78–83. DOI: 10.1109/ASET48392.2020.9118193

Сучасний стан наукових досліджень та технологій в промисловості. 2025. № 3 (33)
ISSN 2522-9818 (print)
ISSN 2524-2296 (online)

29. Wulandari, R., Santoso, A., Nugroho, H. (2021), "Fingerprint Identification Using Edge Detection and GLCM Analysis". *2021 International Conference on Computer Science (ICCS)*, Jakarta, Indonesia, IEEE, P. 123–128. DOI: 10.1109/ICITech50181.2021.9590134
30. Patel, R., Sharma, S. & Kumar, V. (2021), "Technique for Processing Noisy Fingerprints with Extreme Distortions". *2021 International Conference on Computer Systems (ICCS)*, Bangalore, India, IEEE, P. 45–50. DOI: 10.1109/ICCS54944.2021.00068
31. Yu, T., Zhang, X. & Li, Y. (2025), 3D Fingerprint Unwrapping Using B-Spline for 2D Recognition. *IEEE Open Journal of the Computer Society*, Vol. 6, P. 123–134. DOI: 10.1109/OJCS.2025.3559975
32. Calderón-Calderón, M.D., Medina-Pérez, M.A. & Monroy, R. (2025), "Fingerprint Quality Enhancement for Low-Resolution Scanners. *IEEE Access*, Vol. 13, P. 56789–56798. DOI: 10.1109/ACCESS.2025.3527071
33. Pohuliaiev, Y. (2025), "Euclidean fingerprint descriptor and comparator model software". URL: https://drive.google.com/file/d/1bRD2yqc7Zg6NSBpGYvtAVv-hiJrekJJh/view?usp=sharing (last accessed: 01.05.2025)

Надійшла (Received) 03.06.2025

Відомості про авторів / About the Authors

Pohuliaiev Yurii – Postgraduate Student, Kharkiv National University of Radio Electronics, Department of Software Engineering, Kharkiv, Ukraine; e-mail: yurii.pohuliaiev@nure.ua; ORCID ID: https://orcid.org/0009-0005-5883-1661

Smelyakov Kirill – Doctor of Sciences (Engineering), Professor, Head at the Department of Software Engineering, Kharkiv National University of Radio Electronics, Kharkiv, Ukraine; e-mail: kyrylo.smelyakov@nure.ua; ORCID ID: https://orcid.org/0000-0001-9938-5489

Погуляєв Юрій Сергійович – Харківський національний університет радіоелектроніки, аспірант кафедри програмної інженерії, Харків, Україна.

Смеляков Кирило Сергійович – доктор технічних наук, професор, завідувач кафедри програмної інженерії, Харківський національний університет радіоелектроніки, Харків, Україна.

МЕТОД ПОРІВНЯННЯ ВІДБИТКІВ ПАЛЬЦІВ, ЗАСНОВАНИЙ НА МОДЕЛІ ПОПЕРЕДНЬОГО ВИРІВНЮВАННЯ

Предметом статті є розробка та аналіз нового методу порівняння відбитків пальців, що використовує геометричні евклідові характеристики мінуцій для біометричної ідентифікації. Дослідження зосереджується на мінуціях – специфічних точках переривання або роздвоєння папілярних ліній – як ключових біометричних ознаках, протиставляючи їх традиційним глобальним і локальним дескрипторам, таким як SIFT, HOG чи LPQ. **Мета** полягає у розробці стійкого й ефективного методу порівняння відбитків пальців, що використовує геометричні евклідові характеристики мінуцій і попереднє вирівнювання, для підвищення точності біометричної ідентифікації без залежності від машинного навчання. **Завдання** дослідження триетапні: по-перше, дослідити теоретичні основи дескрипторів на основі мінуцій та їхню інваріантність до афінних перетворень (зсув, обертання, масштабування); по-друге, розробити модель із використанням вектора зсуву та функцій відстані для зіставлення мінуцій; по-третє, експериментально перевірити модель, визначивши оптимальні параметри та оцінивши її на стандартному наборі даних. **Методи** охоплюють теоретичний аналіз і експериментальну оцінку. Теоретична основа встановлює стійкість вирівнювання до зсувів. Дескриптор формується через координати мінуцій, функції відстані та оптимізацію зіставлення. Для вилучення ознак застосовано алгоритм обробки зображень із фільтрацією й аналізом мінуцій. **Результати** отримані з допомогою експериментальної перевірки на наборі FVC2000 (DB1_B) демонструють високу продуктивність, яка оцінюється метриками класифікації та часом виконання. **Висновки** підкреслюють теоретичні та практичні надбання дослідження. Модель демонструє теоретичну й практичну стійкість до евклідових зсувів, пропонуючи переваги для обробки відбитків із різних сканерів. Експерименти підтверджують ефективність виявлення зсувів, досягаючи високої міри Ван Різбергена (0.735), хоча залежність від позитивних збігів вимагає додаткової фільтрації помилково позитивних результатів. Метод є робочим і може бути застосований практично.

Ключові слова: дактилоскопія, відбитки пальців, попереднє вирівнювання, мінуції, біометрична ідентифікація, афінні перетворення, тензорне представлення, машинне навчання, FVC2000, метрики бінарної класифікації..

Бібліографічні описи / Bibliographic descriptions

Погуляєв Ю.С., Смеляков К.С. Метод порівняння відбитків пальців, заснований на моделі попереднього вирівнювання. *Сучасний стан наукових досліджень та технологій в промисловості*. 2025. № 3 (33). С. 88–101. DOI: https://doi.org/10.30837/2522-9818.2025.3.088

Pohuliaiev, Y., Smelyakov, K. (2025), "Method for comparing fingerprints based on a previous alignment model", *Innovative Technologies and Scientific Solutions for Industries*, No. 3 (33), P. 88–101. DOI: https://doi.org/10.30837/2522-9818.2025.3.088